



II-VI based organic-inorganic hybrid structures: Brief review and perspective

Yong Zhang

Electrical and Computer Engineering Department, The University of North Carolina at Charlotte, Charlotte, NC, 28223-0001, USA

ARTICLE INFO

Keywords:

Organic-inorganic hybrid
Structural ordering
Long-term stability
II-VI binary
Exciton
Phonon
Superlattice
2D material
Quantum wire
Thermal expansion

ABSTRACT

Translational symmetry is the signature of a crystal. Organic-inorganic hybrid materials can be classified in four levels according to the degree of deviating from this strict definition of the crystal. Among the large number of organic-inorganic hybrid materials, only a small fraction can be considered as crystalline even in a broad sense, whereas most of them are simply non-crystalline or highly disordered, referred to as the first level. Those hybrids that may be considered as crystalline can be categorized into the next three levels. The second level includes those that do not have short-range order but exhibit approximate long-range periodicity, such as the room temperature phase hybrid halide perovskites, resembling semiconductor alloys. The third level comprises those hybrids that behave like a real crystal on macroscopic scale (e.g., with very well defined XRD patterns) nevertheless have considerable amount of microscopic scale defects (e.g., vacancies) and maybe also some extended defects (e.g., dislocations), similar to epitaxially grown GaN. The fourth level is reserved for those not only having very high degree of crystallinity on the macroscopic scale but also very few microscopic or extended defects, similar to Si. The II-VI based hybrids belong to either the third or fourth level. A brief review on the structural and physical properties and long-term stability of II-VI based hybrids are given, illustrated with a few prototype structures, in comparison with their inorganic counterparts and other hybrids. Perspective is given on the future studies of these hybrids.

1. Introduction

Organic-inorganic hybrid materials are of great interest for offering novel and enhanced properties compared to their inorganic and organic counterparts [1–8]. However, most of them exhibit two drawbacks: (1) structural disorder and (2) poor long-term stability. Many of them are simply non-crystalline materials [1]. Some may be considered as crystalline materials in the same sense as semiconductor alloys that are not crystals in the genuine sense, i.e., lack of translational symmetry. For instance, the room temperature phases of the most extensively studied IV-VII₂ based organic-inorganic hybrids, halide perovskites (e.g., MAPbI₃) [9,10]. Some level of disorder is not necessarily bad for some applications, such as solid-state lighting (SSL) or photovoltaics (PV), as long as it does not shorten the carrier diffusion length so badly that the carrier transport along the critical dimension is inhibited (e.g., along the thickness direction in a planar solar cell). In fact, a moderate level of carrier localization can boost light emission efficiency by suppressing non-radiative recombination [11,12], which is ultimately desirable not only for light emitting devices but also for solar cells [13]. However,

disordering diminishes quantum coherence, which is required for various advanced applications, such as quantum optics [14], and affects negatively on many basic material properties, such as exciton dynamics and electronic conductivity [15]. Even those that do appear like real crystalline materials when characterized with macroscopic scale probing techniques, such as X-ray diffraction (XRD) and Raman scattering, many of them still exhibit a large number of microscopic defects, such as many II-VI and I-VII based hybrids [6,8], manifesting as, for instance, extensive below bandgap emission. Only in very rare cases the hybrid materials can have as good or nearly as good crystallinity as simple binary semiconductors. Perhaps the only documented example in the literature is one of the II-VI based hybrid, β -ZnTe(en)_{0.5} [16].

As regarding the long-term stability, we mean a time scale of one or two decades that is typically expected for (opto-)electronic applications. The hybrid perovskites of intense current interest are known to have relatively poor long-term stability, both under ambient conditions [7] and illumination [17], which limits the scope of their applications. Because of their extraordinary performance as emerging PV materials, concerted effort has been devoted to improving their stability. Major

E-mail address: yong.zhang@uncc.edu.

<https://doi.org/10.1016/j.jlumin.2022.118936>

Received 29 November 2021; Received in revised form 9 April 2022; Accepted 27 April 2022

Available online 2 May 2022

0022-2313/© 2022 Elsevier B.V. All rights reserved.

improvement has been demonstrated, from hours just a few years ago [17] to currently up to a couple of months, benefiting from reduction in structural defects and surface passivation [18–20], although it remains inadequate for general applications in PV and SSL. Long-term stability and high melting points of familiar semiconductors like Si and GaAs are intrinsically associated with their large formation energies [21]. However, extrinsic effects, such as surface and defects, often affect their stability under ambient condition. Surface oxidation is practically inevitable for most inorganic semiconductors, such as Si, GaAs, and ZnTe. Fortunately, for most crystalline inorganic materials, the oxidation is usually a self-limiting process, which ensures their long-term stability. One of the II-VI hybrids, β -ZnTe(en)_{0.5}, appears to be the first documented hybrid material with well over one-decade long-term stability, as reported recently by comparing aged and newly synthesized samples [16]. It has been shown that β -ZnTe(en)_{0.5} has a much larger formation energy, in the order of 0.5 eV, compared to that of MAPbI₃ at around -0.1 eV (i.e., spontaneously unstable based on thermodynamics) [22]. Additionally, the former has an additional kinetic barrier, resulting in a total thermodynamic barrier over 1.6 eV, whereas for the latter it likely relies on a yet unknown kinetic barrier to maintain its room temperature stability. Interestingly, the long-lived β -ZnTe(en)_{0.5} samples were also found to have a self-limiting thin oxide layer, although others that appeared degraded under optical characterization had a much thicker oxide layer (~2 μ m) [16]. The variation in aging result

indicates that both intrinsic and extrinsic degradation mechanisms are at work in influencing the long-term stability. This unique example prompts a question: can one indefinitely improve the long-term stability of a material? A similar question has been asked in biology, despite biology systems are perhaps far more complex than semiconductor materials. There is quite obvious variation on the lifespan between species, for instance, dog vs. human [23]. It has also been suggested that there is a fundamental or absolute limit of human lifespan in the range of 120–150 years [24]. If each material does have a finite lifespan dictated by thermodynamics beyond the improvement that can be provided by auxiliary effort, such as surface passivation and eliminating structural defects, would it be prudent to assess the material long-term stability after it shows sign of potential interest for an intended application?

2. II-VI based organic-inorganic hybrid structures

II-VI based organic-inorganic hybrid structures were first reported in 2000 for three structures: α -ZnTe(en)_{0.5}, β -ZnTe(en)_{0.5}, and α -ZnTe(pda)_{0.5}, with their crystal structures determined and optical bandgap estimated [25]. Thereafter, many more II-VI hybrids with group II elements Zn, Cd, and Mn and group VI elements S, Se, and Te have been synthesized, structurally analyzed, and optical bandgap estimated [26–28]. These hybrid structures can be categorized into three groups [28]: as shown schematically in Fig. 1(a), (1) three-dimension (3D) like

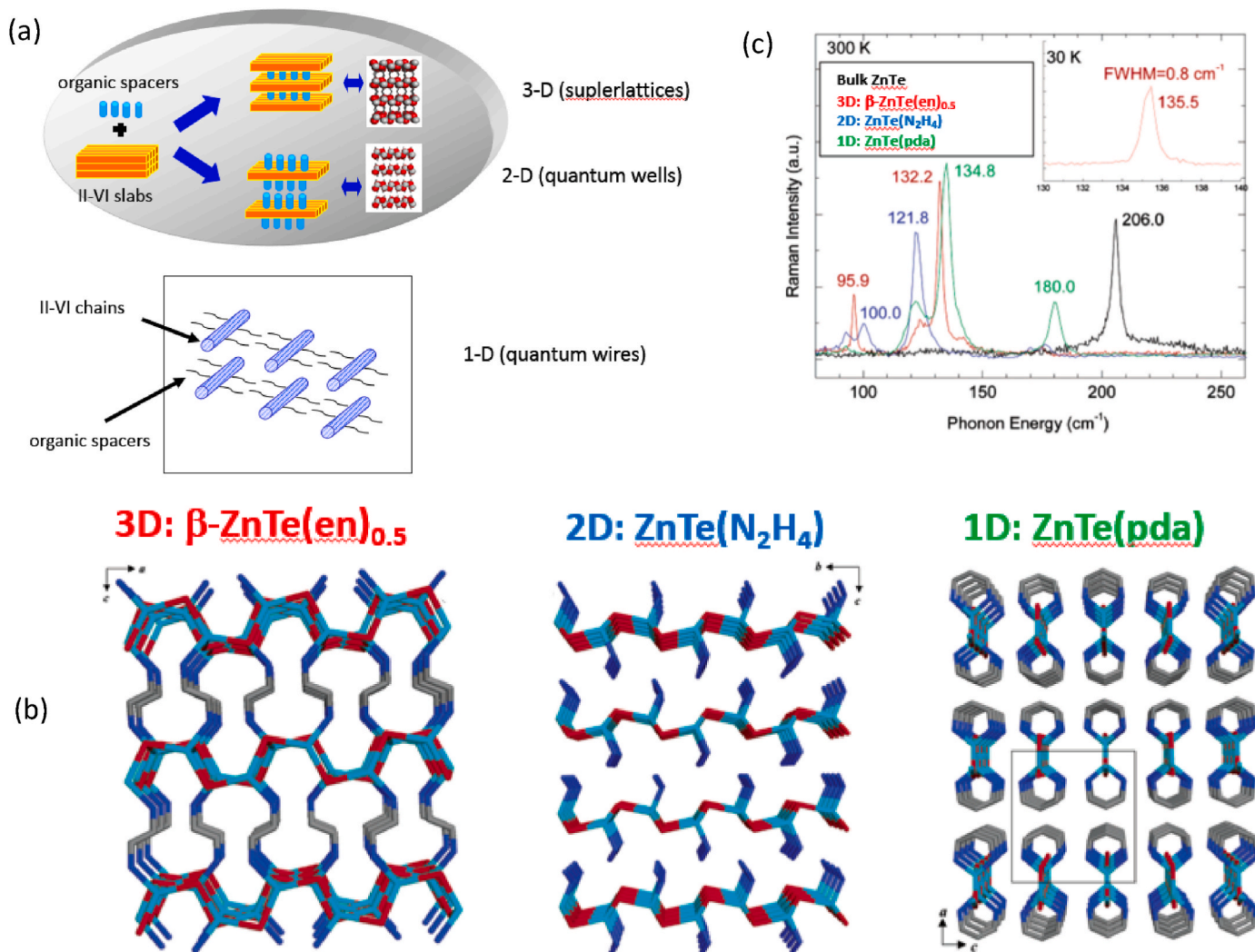


Fig. 1. (a) Schematics of II-VI based hybrids in 3D, 2D, and 1D structures. (b) Crystal structures of prototype 3D, 2D, and 1D structures based on ZnTe. (c) Raman spectra of the three ZnTe hybrid structures and ZnTe. (Panel (a) courtesy of Jing Li; (b) and (c) reproduced with permission [28]).

structures, 3D-(MQ) $L_{0.5}$, where for the β phase two-monolayer thick (110) slabs of a zincblende (ZB) structure (or their wurtzite equivalents for the α phase) are interconnected by organic molecules, for instance, ethylenediamine (en) = $C_2N_2H_8$, forming cation-N bonds. The inorganic layer thickness was sometimes referred to as “single atomic layer” in the literature [27,28], but should instead be “two monolayers”, following the convention of describing the layer thickness in a semiconductor heterostructure. (2) Two-dimension (2D) like structures, 2D-(MQ)L, where only one end of the organic molecule (N) bonds with the cation of the inorganic layer of the same thickness as in the 3D structure, resembling layered structures. In this group, it is also possible to have structures with the inorganic slab thickness doubled, 2D-(M₂Q₂)L, referred to as a “double layered” structure (actually having four monolayers) [29]. (3) One-dimension (1D) like structures, where the single atom thick binary chains of the wurtzite structure bond with the molecules (both ends of the molecule bond to the cation), and an assembly of such quasi 1D structures in parallel form the hybrid crystal. The array has a very high density around 2×10^{14} wires/cm² for 1D-ZnTe(pda). The individual inorganic chains in these 1D structures can be viewed as the smallest quantum wire practically possible. The structure can also be viewed as an atomic chain passivated by a molecule to its cation sites.

Fig. 1(b) compares three ZnTe based hybrid structures, 3D- β -ZnTe(en)_{0.5}, 2D-ZnTe(N₂H₄), and 1D-ZnTe(pda), as examples for 3D, 2D, and 1D structures, respectively [28]. Fig. 1(c) compares their room-temperature Raman spectra together with that of ZnTe [28]. Not only they are very much different from that of ZnTe but also distinctly different from each other. Small Raman linewidths indicate that the hybrid structures possess high crystallinity. Particularly, the low temperature (30 K) spectrum for β -ZnTe(en)_{0.5} shows a linewidth of 0.8 cm⁻¹, comparable to many binary semiconductors (though slightly larger than the highest quality binary, such as GaAs). However, we do want to stress that characterization techniques like XRD and Raman typically do not reflect the degree of structural ordering in microscopic scale (e.g., presence of point defects), thus, cannot predict the material quality relevant to electronic properties. On this regard, some 3D structures, particularly β -ZnTe(en)_{0.5}, are very unique, because at room temperature, not only it shows a clean bandgap exciton emission with nearly no visible below bandgap emission but also very little non-radiative recombination [16]. Together with its very high macroscopic scale structural ordering, with XRD linewidths comparable to many

binary semiconductors (e.g., GaN), β -ZnTe(en)_{0.5} could very well be the most perfect man-made superstructure [16]. Certainly its structural perfectness is far better than any inorganic superlattices, such as GaAs/AlAs [30]. This exceptional level of structural perfectness found in the 3D hybrid structures benefits from its unique structure where the ultra-thin inorganic slab is much less likely to form structural defects, distinctly different bonding arrangements between the inorganic and organic component make it impossible to have the commonly encountered interdiffusion of neighboring components in the inorganic superlattices, and lastly that both ends of the organic molecules are bonded to the inorganic slabs forces the molecules to take one well-defined conformation [31]. The all covalent like bonding [25] also makes the 3D structure more stable than the other structures.

The 2D structures, with one dangling end of the molecule, are found to be highly defective in the sense that they typically exhibit a broad below bandgap emission band. For examples, Fig. 2(a) show PL spectra for a few 2D structures with four-monolayer thick inorganic slabs (also known as “double-layered”): 2D-CdS(ba)_{0.5} ($E_g \sim 2.9$ eV), 2D-CdSe(ba)_{0.5} ($E_g \sim 2.7$ eV), and 2D-ZnS(ba)_{0.5} ($E_g \sim 3.9$ eV) (Y. Zhang, 2004, unpublished results with samples provided by Jing Li). The spectra show broad emission bands much below the respective bandgaps. Although the bandgaps were only estimated from diffuse reflectance measurements using a Kubelka-Munk function [29], they are adequate to conclude that the broad emission bands were not originated from the intrinsic band edge emission. For comparison, PL spectra of 3D- β -ZnTe(en)_{0.5} are shown in Fig. 2(b), where the two spectra were measured respectively from a then newly synthesized sample (S19-p) and an aged sample (S07-p) [16]. The spectra show very little below bandgap emission other than the band edge free exciton emission, in stark contrast to the spectra of the 2D hybrids shown in Fig. 2(a). It is of particularly impressive that the sample synthesized in 2007 stored under the ambient condition remained as pristine as the new sample. It is also important to mention that under UV illumination (325 nm) the photo-stability of the 2D structures CdX(ba)_{0.5} with X = S, Se, and Te decreases with going down the column of the periodic table or increasing the ionicity of the binary. For the Te based structure, the powder sample degraded (PL quenched and illuminated site tuning dark) almost instantly when illuminated by 325 nm laser. The photo-stability was slightly better for the Se version, but the S version was found quite stable. However, 2D-ZnS(ba)_{0.5} was found furthermore stable. This trend seems to be consistent with the relative stability of

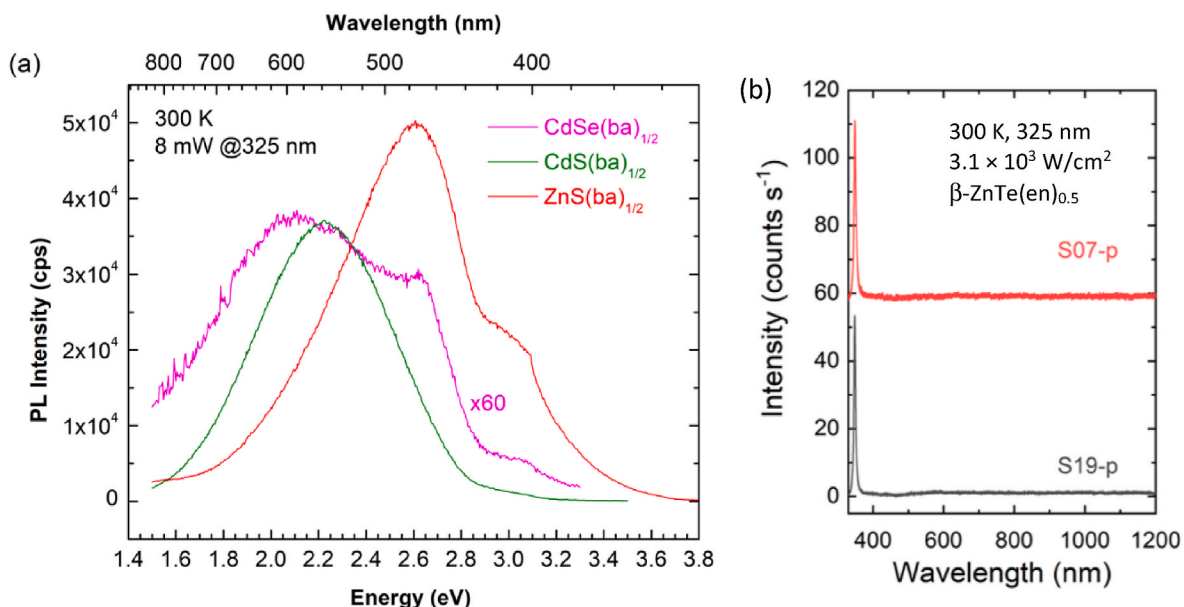


Fig. 2. (a) PL spectra of 2D-(MQ) $L_{0.5}$. (b) PL spectra of 3D- β -ZnTe(en)_{0.5}.

MAPbX₃ with X = Cl, Br, and I. Although the exact nature of the below bandgap emission remains unknown, the broad emission band shown in Fig. 2(a) has motivated the use of 2D-CdS(ba)_{0.5} as phosphor for white light emission excited by a UV light LED [32].

So far, detailed material property studies have been performed mostly on selected 3D structures, mostly on 3D-β-ZnTe(en)_{0.5}, because of their highly ordered structures as well as better stability. Below we offer a brief summary of the work related to the 3D structures and offer some perspective for the future studies.

3. A brief review and perspective on 3D-(MQ)L_{0.5}

Despite very limited effort on selected structures, the II-VI based hybrid structures have been demonstrated to be unique in a number of ways not only in the organic-inorganic hybrid materials but also in semiconductor materials in general. Almost any property being investigated, something unusual has been observed. A few examples are given below mostly from the studies on a few prototypes belonging to the group 3D-[MQ](L)_{0.5}.

- 1) **Long-term stability** β-ZnTe(en)_{0.5} is the first documented organic-inorganic hybrid structure with shelf life well over 10 years, and the first hybrid structure with its intrinsic thermal degradation barrier (consisting of thermodynamic barrier and kinetic barrier) being experimentally measured with a projected intrinsic half-life over 10⁸ years [16]. This result was obtained by measuring the time decay of Raman signal intensity in N₂ environment at elevated temperatures between 210 °C and 270 °C. Similar measurement in air will offer the information for the intrinsic shelf life for the structure when there is no unintended structural defect other than the naturally formed surface oxide layer.
- 2) **Free exciton emission and absorption** β-ZnTe(en)_{0.5}, as a biaxial crystal, is typically obtained as a single-crystalline platelet with the platelet normal along the *b* axis or the organic-inorganic stacking direction. It is anisotropic between the two in-plane axes *a* and *c*, with the *a* axis being equivalent to the (001) axis of the ZB ZnTe and the *c* axis the [110] of the ZB ZnTe. At 1.5 K, the band edge excitonic absorption peak at 3.7192 eV exhibits an absorption coefficient of around 300 cm⁻¹ with the *a*-polarization, and around 1,100,000 cm⁻¹ with the *c*-polarization [33], which is among the strongest band-edge excitonic absorption reported in semiconductors [34]. For ZnTe, the value is around 140,000 cm⁻¹. The corresponding excitonic or exciton-polariton emission peak is found at 3.7193 eV [33]. This practically exact match with the absorption peak, within the uncertainty, could be the first unambiguous observation of free exciton emission in an organic-inorganic hybrid semiconductor. Other more casual claims of free exciton emission in the hybrids might find the emission peak energy being within 10 meV of the absorption peak [34]. Although one cannot preclude that the Stokes-shifted emission peak was indeed free exciton emission, impurity and defect emission might also appear in the vicinity of the fundamental bandgap, as known in many inorganic semiconductors.
- 3) **Zero and negative thermal expansion** Usually, negative thermal expansion is of interest to counterbalance positive thermal expansion, which is more commonly observed in semiconductor or insulating materials, to achieve zero-thermal expansion. Most materials that exhibit negative thermal expansion are oxides [35]. The 3D hybrids (ZnTe)₂C_nN₂H_{2n+4} (*n* = 0, 2–5) are the first non-oxide semiconductors showing zero or negative thermal expansion [36,37]. Significantly, these examples offer a novel approach for thermal expansion design and tuning.
- 4) **Structural perfectness** Ever since the concept of semiconductor superlattices was proposed by Esaki and Tsu in 1970 [38], the holy grail of nanoscale assembling has been to achieve a super-structure consists of nanoscale units of identical physical size and chemical composition, arranged in an ordered manner with genuine translational symmetry. However, this dream has turned out to be much more difficult to realize than one might anticipate. For instance, for the best investigated system, GaAs/AlAs superlattices, because of the close similarity between the constituents Ga and Al, atomic inter-diffusion within a few monolayers of the interface is practically inevitable [30], which makes a perfect superlattice non-achievable after five decades. β-ZnTe(en)_{0.5} may very well be the most perfect man-made superlattice, with macroscopic scale structural ordering (e.g., measured by XRD and Raman) as good as most binary semiconductors (e.g., GaN) [16,28,36]; and microscopic scale structural ordering much better than any known semiconductors, including GaAs, CdTe, and hybrid perovskite [10], with nearly 100% room temperature photoluminescence internal quantum efficiency over 6 orders in excitation density [16]. Although slightly worse than those most mature elementary and binary semiconductors, such as Si and GaAs, in terms of the macroscopic structural parameters (e.g., XRD linewidth), given the complexity of the hybrid (β-ZnTe(en)_{0.5} consists of 32 atoms/unit cell), the results for the hybrid are in fact very impressive. Considering both macroscopic and microscopic scale defects, overall the hybrid β-ZnTe(en)_{0.5} is among the structurally most perfect semiconductors reported.
- 5) **Potential as p-type transparent conductive materials** No stable p-type transparent conductive (TC) material is currently available, while p-TC materials are universally desired to have for all (opto)electronic devices. With room temperature bandgaps over 3.5 eV, the advantageous conduction band and valance band alignments of β-ZnTe(en)_{0.5} relative to other better known high bandgap materials, such as ITO, ZnO, GaN, make it potentially a very promising candidate for p-type TC material [33]. The underlying physics lies in that the acceptor binding energy is positively correlated to the atomic energy level difference between the dopant and host atom that dominates the valance band states rather than determined by the Coulomb potential as commonly thought [39]. Therefore, a semiconductor with a high valance band maximum (VBM) energy level is more likely to have effective p-type doping, which is why ZnTe can achieve the highest p-type conductivity among all II-VI semiconductors because of its highest VBM, whereas ZnO is the most difficult to achieve effective p-type doping because of its O p-state derived VBM being very low. β-ZnTe(en)_{0.5} can potentially be doped with group I elements Cu and Ag to become p-type conductive.
- 6) **Unusual elastic properties** Elastic constants C_{ij} of β-ZnTe(en)_{0.5} have been calculated using density-functional theory (DFT) [40]. The elastic response of the hybrid is unsurprised to be highly anisotropic. For instance, if (x,y,z) is assumed to match the (b,a,c) axes of the crystal, the Poisson's ratios can be calculated using the reported C_{ij} values, which yields ν_{zx} = -0.0111 and ν_{xz} = -0.0098, indicating small but negative Poisson's ratios for stretching along z (*c* axis) and along x (*b* axis), respectively; ν_{yx} = 0.2740 and ν_{xy} = 0.4393, ν_{yz} = 0.3095 and ν_{zy} = 0.5586, showing normal positive Poisson's ratios, albeit anisotropic. For bulk ZnTe, ν = 0.3533. Also found is that the hybrid has strongly enhanced shear response, about a factor of 5 as large, for the zx component compared to the bulk ZnTe. It means that a small shear stress along the *c* axis on the *b* plane can lead to a large distortion on the structure, which is understandable because along the *c* axis the inorganic slab is most rigid and the molecules are aligned perpendicular to the *c* axis [16]. These properties are yet to be confirmed experimentally and potentially can be used for high sensitivity stress sensing applications.
- 7) **Stacked quasi 2D sheets** Quasi 2D materials, monolayer MoS₂ and alike, have many interesting properties. However, a single

monolayer cannot offer adequate volume effect, for instance, optical absorption for certain applications (e.g., photo-detection). Attempting to stack them directly will result in drastic change in the material properties, despite it might be desirable for some applications [41]. It is thus highly desirable to be able to stack as many quasi 2D sheets as needed yet with minimal changes in the basic material properties. One could in principle overcome the issue by inserting a thin insulating layer (e.g., BN) in between the monolayers (a superlattice like structure), but so far this approach can only be done manually for a limited number of stacks [42]. It would be highly desirable to have a 2D like material that has a sizable bandgap and can be stacked in an arbitrary number of layers as needed, with precisely controllable inter-layer coupling and thus material properties. Hybrid structures, such as 3D hybrids $(\text{ZnTe})_2\text{C}_n\text{N}_2\text{H}_{2n+4}$ ($n = 0, 2-5$), could be the options for this purpose. The spacing between the inorganic slabs can be turned approximately from 4 to 10 Å to fine tune the electronic coupling between the inorganic slabs. This possibility offers unique opportunity to investigate the collective effects of electronically weakly coupled ultra-thin semiconductor layers, without the extreme sensitivity of the layer number dependence in systems like MoS_2 .

- 8) **Room temperature exciton-polariton condensation** Large exciton binding energies (>200 meV), sharp excitonic resonance (due to very high crystallinity), and excellent stability offer the II-VI hybrids unique advantages over other systems. The sharp resonance requires low energy input, and the high ordering ensures long quantum coherence time. Exciton binding energy for $\beta\text{-ZnTe}(\text{en})_{0.5}$ was estimated using effective mass theory [33], which is unlikely accurate for this type of system with the anticipated large exciton binding energy. A more rigorous theory, GW based approach solving Bethe-Salpeter equation, is required to offer accurate understanding of the excitonic properties in these hybrids. Exciton-polariton effects can be explored in the similar manner as other less ordered hybrids [43].
- 9) **Phonon-polariton** $\beta\text{-ZnTe}(\text{en})_{0.5}$ is perhaps the first semiconductor superlattice of which all Raman modes can be unambiguously identified [16], in contrast to the other semiconductor superlattices known today (e.g., GaAs/AlAs), none of which has a Raman spectrum free of ambiguity in the assignments to at least some of its Raman modes due to inevitable structural fluctuations [44]. The structural perfection of the II-VI hybrids allows for the study of the phonon-polariton effects having a clean starting point. Many expected Raman modes of $\beta\text{-ZnTe}(\text{en})_{0.5}$ have been identified by comparing with DFT calculated Raman mode frequencies and symmetries [16]. Polarized Raman spectra remain to be analyzed and compared with the calculated Raman tensors. Phonon polariton effects can then be explored.
- 10) **Carrier mobility** It has been shown that even along the inorganic/organic stacking direction, $\beta\text{-ZnTe}(\text{en})_{0.5}$ exhibits a mobility close to $10^{-2} \text{ cm}^2/(\text{V s})$ at room temperature [16], which is much better than the bulk mobilities in most semiconducting organic materials. It can be further enhanced by changing the spacer molecule. The in-plane mobility has been measured to be around $100 \text{ cm}^2/(\text{Vs})$ (Zhang group, unpublished), which is as good as inorganic semiconductors like GaN and CdTe. These results ensure the feasibility of practical applications of these materials.
- 11) **UV device applications** UV light emitting and detecting devices can benefit from the ultra-strong band edge absorption and oscillator strength. The transparency to the full visible spectrum can be utilized for fabricating transparent electronic devices (e.g., transistors and sensors).
- 12) **Thermoelectric application** $\beta\text{-ZnTe}(\text{en})_{0.5}$ has been predicted, although not yet measured, to have roughly a factor of 10 reduction in thermal conductivities [40]. Coupling with the

measured high carrier mobility (much better than most thermoelectric materials), the 3D II-VI hybrids are of great interest for exploring thermoelectric applications.

4. Summary

II-VI based organic-inorganic hybrids are unique in many ways compared to most known hybrid materials. Although a large number of structures have been synthesized together with their basic material properties characterized, they remain largely unexplored, as another family of the hybrid materials beyond the hybrid perovskites. We hope that this brief review and perspective can provide insights for others to see the similarity and distinction between these II-VI hybrids and other hybrids as well as inorganic semiconductors, and to stimulate further investigation on their physical and chemical properties and exploration in practical applications.

Declaration of competing interest

The authors declare that they have no known competing financial interests or personal relationships that could have appeared to influence the work reported in this paper.

Acknowledgement

I would like to thank all my collaborators at Rutgers University, NREL, UNC-Charlotte, and other institutes who have contributed to the work mentioned in this paper. The work at UNC-Charlotte was supported by ARO/Physical Properties of Materials Program (Grant No. W911NF-18-1-0079), and Bissell Distinguished Professorship.

References

- [1] H.S. Nalwa, Handbook of Organic-Inorganic Hybrid Materials and Nanocomposites, American Scientific Publishers, 2003.
- [2] T. Ishihara, Optical properties of Pb-based inorganic-organic perovskites, in: T. Ogawa, Y. Kanemitsu (Eds.), Optical Properties of Low-Dimensional Materials, World Scientific, Singapore, 1995, pp. 289–339.
- [3] D.B. Mitzi, Synthesis, structure, and properties of organic-inorganic perovskites and related materials, in: Karlin (Ed.), Progress in Inorganic Chemistry, John Wiley & Sons, Inc., 1999, pp. 1–121.
- [4] C. Sanchez, State of the art developments in functional hybrid materials, *J. Mater. Chem.* 15 (2005) 3557–3558.
- [5] G. Kickelbick, Hybrid Materials, Wiley-VCH Verlag GmbH & Co. KGaA, 2007.
- [6] J. Li, R. Zhang, A new class of nanostructured inorganic-organic hybrid semiconductors based on II-VI binary compounds, *Prog. Inorg. Chem.*, pp. 445–504.
- [7] M. Gratzel, The light and shade of perovskite solar cells, *Nat. Mater.* 13 (2014) 838–842.
- [8] W. Liu, Y. Fang, J. Li, Copper iodide based hybrid phosphors for energy-efficient, *Gen. Lighting Technol.* 28 (2018) 1705593.
- [9] A. Poglitsch, D. Weber, Dynamic disorder in methylammoniumtrihalogenoplumbates (II) observed by millimeter-wave spectroscopy, *J. Chem. Phys.* 87 (1987) 6373–6378.
- [10] F. Zhang, J.F. Castaneda, S. Chen, W. Wu, M.J. DiNezza, M. Lassise, W. Nie, A. Mohite, Y. Liu, S. Liu, D. Friedman, H. Liu, Q. Chen, Y.-H. Zhang, J. Huang, Y. Zhang, Comparative studies of optoelectrical properties of prominent PV materials: halide perovskite, CdTe, and GaAs, *Mater. Today* 36 (2020) 18–29.
- [11] Y. Zhang, M.D. Sturge, K. Kash, B.P. van der Gaag, A.S. Gozdz, L.T. Florez, J. P. Harbison, Temperature dependence of luminescence efficiency, exciton transfer, and exciton localization in $\text{GaAs}/\text{Al}_x\text{Ga}_{1-x}\text{As}$ quantum wires and quantum dots, *Phys. Rev. B* 51 (1995) 13303.
- [12] S.F. Chichibu, A.C. Abare, M.P. Mack, M.S. Minsky, T. Deguchi, D. Cohen, P. Kozodoy, S.B. Fleischer, S. Keller, J.S. Speck, J.E. Bowers, E. Hu, U.K. Mishra, L. A. Coldren, S.P. DenBaars, K. Wada, T. Sota, S. Nakamura, Optical properties of InGaN quantum wells, *Mater. Sci. Eng., B* 59 (1999) 298–306.
- [13] O.D. Miller, E. Yablonovitch, S.R. Kurtz, Strong internal and external luminescence as solar cells approach the shockley-queisser limit, *IEEE J. Photovoltaics* 2 (2012) 303–311.
- [14] D. Sanvitto, S. Kena-Cohen, The road towards polaritonic devices, *Nat. Mater.* 15 (2016) 1061–1073.
- [15] R.J. Elliott, J.A. Krumhansl, P.L. Leath, The theory and properties of randomly disordered crystals and related physical systems, *Rev. Mod. Phys.* 46 (1974) 465–543.
- [16] T. Ye, M. Kocherga, Y.-Y. Sun, A. Nesmelov, F. Zhang, W. Oh, X.-Y. Huang, J. Li, D. Beasock, D.S. Jones, T.A. Schmedake, Y. Zhang, II-VI Organic-Inorganic

- hybrid nanostructures with greatly enhanced optoelectronic properties, perfectly ordered structures, and shelf stability of over 15 years, *ACS Nano* 15 (2021) 10565–10576.
- [17] Q. Chen, H. Liu, H.-S. Kim, Y. Liu, M. Yang, N. Yue, G. Ren, K. Zhu, S. Liu, N.-G. Park, Y. Zhang, Multiple-stage structure transformation of organic-inorganic hybrid perovskite $\text{CH}_3\text{NH}_3\text{PbI}_3$, *Phys. Rev. X* 6 (2016), 031042.
- [18] S. Yang, S. Chen, E. Mosconi, Y. Fang, X. Xiao, C. Wang, Y. Zhou, Z. Yu, J. Zhao, Y. Gao, F. De Angelis, J. Huang, Stabilizing halide perovskite surfaces for solar cell operation with wide-bandgap lead oxysalts, *Science* 365 (2019) 473–478.
- [19] R. Wang, J. Xue, K.-L. Wang, Z.-K. Wang, Y. Luo, D. Fenning, G. Xu, S. Nuryyeva, T. Huang, Y. Zhao, J.L. Yang, J. Zhu, M. Wang, S. Tan, I. Yavuz, K.N. Houk, Y. Yang, Constructive molecular configurations for surface-defect passivation of perovskite photovoltaics, *Science* 366 (2019) 1509–1513.
- [20] Y. Wang, T. Wu, J. Barbaud, W. Kong, D. Cui, H. Chen, X. Yang, L. Han, Stabilizing heterostructures of soft perovskite semiconductors, *Science* 365 (2019) 687–691.
- [21] C. Kittel, *Introduction to Solid State Physics*, eighth ed., John Wiley & Sons, 2005.
- [22] Y.-Y. Zhang, S. Chen, P. Xu, H. Xiang, X.-G. Gong, A. Walsh, S.-H. Wei, Intrinsic instability of the hybrid halide perovskite semiconductor $\text{CH}_3\text{NH}_3\text{PbI}_3$, *Chin. Phys. Lett.* 35 (2018), 036104.
- [23] T. Wang, J. Ma, A.N. Hogan, S. Fong, K. Licon, B. Tsui, J.F. Kreisberg, P.D. Adams, A.-R. Carvunis, D.L. Bannasch, E.A. Ostrander, T. Ideker, Quantitative translation of dog-to-human aging by conserved remodeling of the DNA methylome, *Cell Syst.* (2020), <https://doi.org/10.1016/j.cels.2020.06.006>.
- [24] T.V. Pyrkov, K. Avchaciov, A.E. Tarkhov, L.I. Menshikov, A.V. Gudkov, P. O. Fedichev, Longitudinal analysis of blood markers reveals progressive loss of resilience and predicts human lifespan limit, *Nat. Commun.* 12 (2021) 2765.
- [25] X.Y. Huang, J. Li, H.X. Fu, The first covalent organic-inorganic networks of hybrid chalcogenides: structures that may lead to a new type of quantum wells, *J. Am. Chem. Soc.* 122 (2000) 8789–8790.
- [26] H.R.I. Heulings, X.Y. Huang, J. Li, Mn-substituted inorganic-organic hybrid materials based on ZnSe: nanostructures that may lead to magnetic semiconductors with a strong quantum confinement effect, *Nano Lett.* 1 (2001) 521–525.
- [27] X.Y. Huang, H.R.I. Heulings, L. Vina, L. Jing, Inorganic-organic hybrid composites containing MQ (II-VI) slabs: a new class of nanostructures with strong quantum confinement and periodic arrangement, *Chem. Mater.* 13 (2001) 3754–3759.
- [28] X.Y. Huang, J. Li, Y. Zhang, A. Mascarenhas, From 1D chain to 3D network: tuning hybrid II-VI nanostructures and their optical properties, *J. Am. Chem. Soc.* 125 (2003) 7049–7055.
- [29] X.Y. Huang, J. Li, From single to multiple atomic layers: a unique approach to the systematic tuning of structures and properties of inorganic-organic hybrid nanostructured semiconductors, *J. Am. Chem. Soc.* 129 (2007) 3157–3162.
- [30] J.H. Li, S.C. Moss, Y. Zhang, A. Mascarenhas, L.N. Pfeiffer, K.W. West, W.K. Ge, J. Bai, Layer ordering and faulting in $(\text{GaAs})_n/(\text{AlAs})_n$ ultrashort-period superlattices, *Phys. Rev. Lett.* 91 (2003) 106103.
- [31] C.Y. Moon, G.M. Dalpian, Y. Zhang, S.H. Wei, Study of phase selectivity of organic-inorganic hybrid semiconductors, *Chem. Mater.* 18 (2006) 2805–2809.
- [32] W. Ki, J. Li, A semiconductor bulk material that emits direct white light, *J. Am. Chem. Soc.* 130 (2008) 8114–8115.
- [33] Y. Zhang, G.M. Dalpian, B. Fluegel, S.-H. Wei, A. Mascarenhas, X.Y. Huang, J. Li, L. W. Wang, Novel approach to tuning the physical properties of organic-inorganic hybrid semiconductors, *Phys. Rev. Lett.* 96 (2006), 026405-026404.
- [34] X. Hong, T. Ishihara, A.V. Nurmikko, Dielectric confinement effect on excitons in PbI_4 -based layered semiconductors, *Phys. Rev. B* 45 (1992) 6961–6964.
- [35] E. Liang, Q. Sun, H. Yuan, J. Wang, G. Zeng, Q. Gao, Negative thermal expansion: mechanisms and materials, *Front. Phys.* 16 (2021) 53302.
- [36] Y. Zhang, Z. Islam, Y. Ren, P.A. Parilla, S.P. Ahrenkiel, P.L. Lee, A. Mascarenhas, M. J. McNevin, I. Naumov, H.X. Fu, X.Y. Huang, J. Li, Zero thermal expansion in a nanostructured inorganic-organic hybrid crystal, *Phys. Rev. Lett.* 99 (2007) 215901–215904.
- [37] J. Li, W.H. Bi, W. Ki, X.Y. Huang, S. Reddy, Nanostructured crystals: unique hybrid semiconductors exhibiting nearly zero and tunable uniaxial thermal expansion behavior, *J. Am. Chem. Soc.* 129 (2007), 14140–+.
- [38] L. Esaki, R. Tsu, *IBM Res. Dev.* 14 (1970) 61.
- [39] Y. Zhang, J. Wang, Bound exciton model for an acceptor in a semiconductor, *Phys. Rev. B* 90 (2014) 155201.
- [40] X. Qian, X. Gu, R. Yang, Anisotropic Thermal Transport in Organic-Inorganic Hybrid Crystal $\beta\text{-ZnTe}(\text{en})_{0.5}$, *J. Phys. Chem. C* 119 (2015) 28300–28308.
- [41] H. Zhang, Ultrathin two-dimensional nanomaterials, *ACS Nano* 9 (2015) 9451–9469.
- [42] Y. Liu, N.O. Weiss, X. Duan, H.-C. Cheng, Y. Huang, X. Duan, Van der Waals heterostructures and devices, *Nat. Rev. Mater.* 1 (2016) 16042.
- [43] G. Lanty, A. Bréhier, R. Parashkov, J.S. Lauret, E. Deleporte, Strong exciton-photon coupling at room temperature in microcavities containing two-dimensional layered perovskite compounds, *New J. Phys.* 10 (2008), 065007.
- [44] B. Jusserand, M. Cardona, Raman spectroscopy of vibrations in superlattices, in: M. Cardona, G. Güntherodt (Eds.), *Light Scattering in Solids*, Springer, Berlin, 1989, p. 49.